Assessment of freezing effects and diagnostic potential of BioBank healthy and neoplastic breast tissues through HR-MAS NMR spectroscopy

test of the integrated areas showed that Cho is significantly different ($p < 0.0002$) when 1 and 12 months and 6 and 12 months classes are compared, whereas Tau ($p < 0.05$) when the comparison is between 1 and 12 months classes.

On the whole, the changes over time of Cho and PC signals in frozen tissues represent not a trivial finding, since many studies base the distinction between neoplastic and healthy tissues or the assessment of tumor grade on the analysis of choline metabolites.

3.4. Comparison between healthy and neoplastic CPMG spectra

The second goal of this work was to verify if, for breast tissues obtained through the Modena BioBank protocol, the metabolic information related to healthy/neoplastic state remains encoded in CPMG spectra, despite the relatively high temperatures experienced by the samples collected through the BioBank before freezing (with respect to those snap-frozen in liquid nitrogen in the operating theater).

All the spectra of the healthy class were compared to all those of the neoplastic one. The *t* test run on the metabolite region of the spectra of the two classes indicates that statistically significant differences ($-\mathrm{Log}(p) > 5$) are found, especially when Cho, PC, Tau, Myo, Lac, Asc, PE and Glc signals are concerned (Fig. S5).

Applying the PCA approach it can be seen that neoplastic and healthy samples cluster, as is shown in Fig. 4a.

Fig. 4

a Scores plot (*left*) of PCA on neoplastic (*green*) versus healthy (*red*) samples. Loadings profiles (*right*) of PC2 and PC3. **b** PLS-DA 3D score plot (*left*) of neoplastic (*green*) versus healthy (*red*) samples. Loading profile (*right*) of the first latent variable (*LV1*)

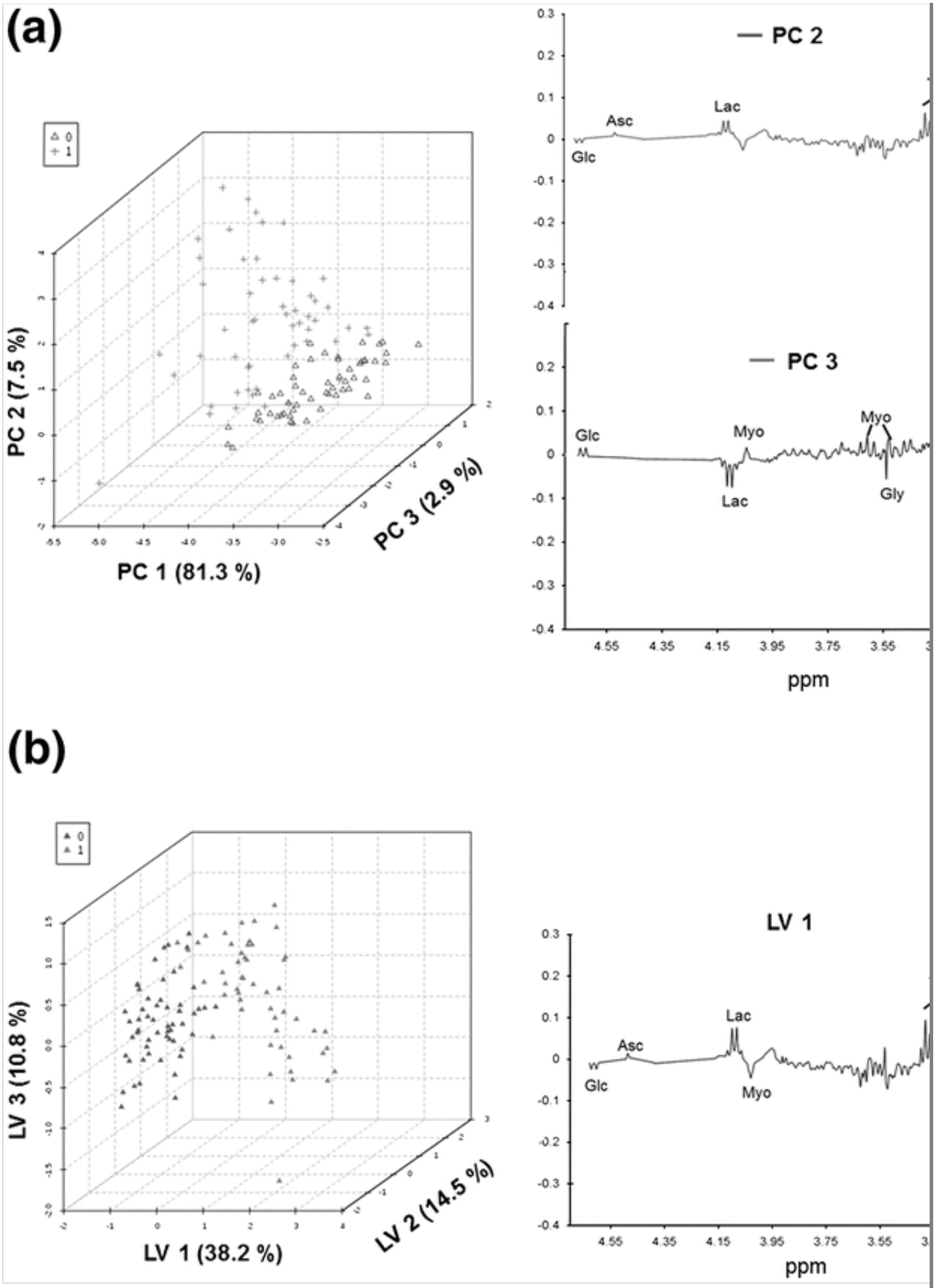

The first three PCs account for 91.7 % of the total variance, and another 1.8 % is captured by PC4 which is dominated by X signal (Fig. S6). Neoplastic samples have PC2 values higher than those of the healthy ones,

i.e. should have at least higher PC, Tau, Lac, PE, Cr and Asc signals and lower Myo, X and β-Glc.

PLS-DA was also run with Metaboanalyst, obtaining a good discrimination between the two classes (Fig. 4b). The optimal number of components, three, was determined through ~~ten~~10-fold cross validation (Fig. S7). To assess the significance of class discrimination, a permutation test was performed (Fig. S7). In each permutation, a PLS-DA model was built between the data and the permuted class labels using the optimal number of components determined by cross validation for the model based on the original class assignment.

PLS-DA loadings profile is very close to that of PC2 in Fig. 4a. It indicates the enhancement of Lac, Tau, PE, PC, Cr and Asc, and to the decreasing of X, Glc and Myo in the neoplastic samples with respect to the healthy ones.

To verify these results of multivariate analysis, integrated areas of the previously selected signals where compared and a ROC analysis (Xia et al. 2012b) was undertaken.

3.5. Analysis of integrals in healthy and neoplastic samples

PCA and PLS-DA point to some metabolites for the distinction of healthy and neoplastic classes, and the signals of these metabolites were integrated after normalization.

When Glc, Asc, Lac, Myo, Tau, PC, Cho, E, PE and Cr integrals were compared (Fig. 5a), it was observed that the differences between all the mean values of healthy and neoplastic distributions are significant at a p level <0.0003, except for Cr ($p = 0.8$) and E ($p = 0.05$).

Fig. 5

a *Bar plots* showing the integrals (mean ± SD) of selected metabolite signals. **b** ROC curve analysis of integrals of selected metabolites in healthy (0) and neoplastic (1) samples. **c** ROC curve analysis of combinations of integrals of selected metabolites in healthy (0) and neoplastic (1) samples. *Red dot* optimal cut-off levels (sensitivity, 1-specificity) and AUC ROC (95 % confidence interval) are also reported

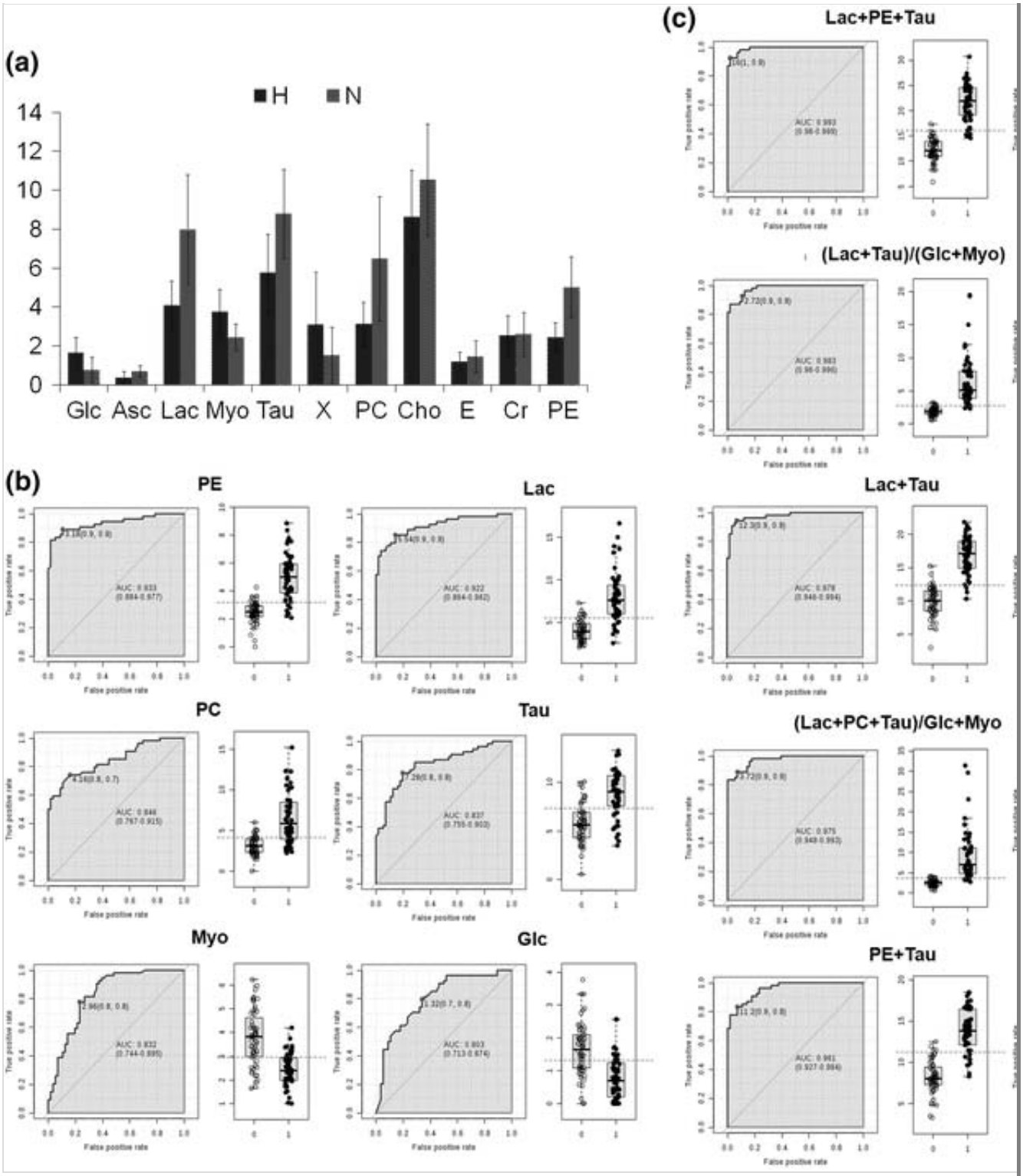

ROC analysis of integrals of the same metabolites (Fig. 5b) confirmed that those more promising for a classification of breast tissue are PE, Lac, PC, Myo, Tau and Glc for which area under ROC curves (AUC) is above 0.8 (Xia et al. 2012b). Also some metabolites combinations (Fig. 5c) seem to be useful for a classification. They were built combining the metabolites with the highest AUC that enhance in neoplastic tissue (PE, Lac, PC and Tau) and in healthy tissue (Glc and Myo). We tried also ratios, that are self-normalized quantities and simplify the use of integrals.

The ROC results point to PE (−Log(p) = 16.1), Lac (−Log(p) = 13.1), and to some of their combinations with other metabolites as good indexes for the healthy/neoplastic classification. In particular, Lac + Tau (−Log(p) = 26.3), Lac + PE + Tau (−Log(p) = 27.9), PE + Tau (−Log(p) = 21.8), and the ratios PE + Tau/Glc + Myo (−Log(p) = 10.4), Lac + Tau/Glc + Myo (−Log(p) = 10.8), Lac + PE + Tau/Glc + Myo (−Log(p) = 11.1) seem promising combinations of biomarkers. Moreover, the ratios are confined in very narrow intervals for healthy samples, whereas they are found in wider and fairly distinguished ranges for the neoplastic ones.

All of these metabolites are reported to be involved in cancer metabolism. An increased consumption of glucose and high accumulated levels of lactate in tumor samples are consistent with the Warburg effect. (Warburg 1956; Vander Heiden et al. 2009). Hypoxia, inadequate oxygen supply to the cells, is frequently found in solid malignant tumors and is characterized by enhanced formation of Lac produced by anaerobic glycolysis. (Warburg 1956). Lower Glc combined with higher Lac levels in cancer patients indicate a difference in glycolytic activity between the two groups. High Lac levels have been shown to correlate with malignancy, increased risk of radiation resistance, metastasis, and reduced recurrence-free and overall survival in several types of cancers. (Tripathi et al. 2012, 2013; Quennet et al. 2006; Brizel et al. 2001; Walenta et al. 2000; Cheng et al. 1998).

The ChoCC are of high interest in cancer research and abnormal choline metabolism is frequently observed. (Tripathi et al. 2012, 2013; Glunde et al. 2011). Samples with high tumor cell content have higher levels of ChoCC compared to healthy samples, with PC being especially elevated in tumors. This reflects the increased proliferation rate in tumors, as Cho is an important constituent of cell membranes through the formation of phosphatidylcholine (PtdCho); PC and GPC are considered precursors and breakdown products of this activity. (Ackerstaff et al. 2003; Esmaeili et al. 2014). The abnormal PC and GPC levels in cancer have been linked to altered enzyme activity, in particular of choline kinase (ChoK) and several phospholipases. (Glunde et al. 2011; Podo 1999). In mammals, ChoK is encoded by two separate genes: ChoKA and ChoKB, catalyzing the phosphorylation of Cho to PC. (Aoyama et al. 2004). The activity of these enzymes depends on oncogenic signaling and microenvironmental parameters such as hypoxia. (Jiang et al. 2012).

Also PE is precursor of the cell membrane phosphatidylethanolamine (PtdEtn), and it is formed by degradation of PtdEtn by phospholipase C. PE has been linked to cancer (Podo 1999) and a recent study on breast cancer has reported that PE induces apoptosis directly through the mitochondrial pathway, leading to a disruption of mitochondrial membrane potential followed by a release of Cytochrome *c* from mitochondria. Furthermore, the arrest at the G1 phase of the cell cycle is in accordance with the observed decrease in Cyclin D1 expression, strongly supporting that PE has a dual mechanism of action i.e. it induces apoptosis and blocks the cell cycle in MCF-7 tumor cells. (Ferreira et al. 2013). Hence, PE has been proposed as anticancer compound.

Elevated level of Tau, osmolite involved in many essential biological functions such as antioxidation, membrane stabilization, and cell shrinkage during apoptosis, should indicate that it is implicated in breast cancer metabolism. (Choi et al. 2012). Choi study showed higher concentrations of Tau and Gly being associated with progesterone receptor (PR) negative/receptor for human epidermal growth factor (HER2) positive cancers and with a poor prognosis.

As for Gly, we observed only a slight increase in neoplastic samples with respect to the healthy ones whereas in previous reports it has been found to contribute to characterization of breast cancer tissues. (Jain et al. 2012; Cao et al. 2012; Sitter et al. 2006). Jain et al. (2012) identified the correlation of Gly with rapid cancer cell proliferation, and that a higher expression of the mitochondrial Gly biosynthesis pathway is associated with higher mortality in breast cancer patients. High levels of Gly and Lac in breast cancer tissues might potentially be associated with high grade malignancy and tumor aggressiveness probably caused by altered glycolysis. (Peeling and Sutherland 1992; Cao et al. 2012). Sitter et al. (2006) reported that Gly concentrations were significantly higher in breast cancers larger than 2 cm compared to those of smaller ones. Hence, since only 8 out of 22 samples here studied were larger than 2 cm, we believe that the slight increase of Gly in the neoplastic samples could be related to the small tumor dimensions and to the early diagnosis.

AQ2

4. Conclusions

The samples collected through Modena BioBank have a thermal history different with respect to that of samples snap frozen in liquid nitrogen immediately after surgery, for the time elapsed between surgery and freezing is around 30 min. During this time, only some metabolic changes have been observed for rat brain cortex (Opstad et al. 2008) or liver (Cacciatore et al. 2013). In particular, significant changes have been observed for Lac, alanine (Ala), γ-aminobutyric acid and Glc in the case of rat brain, and for aspartate and Gly in human liver in the first 30 min after sample excision. When our spectra are compared to those reported by Bathen et al. (2013); and Li et al. (2011) who immediately froze tissues in liquid nitrogen after excision or biopsy, we can hardly infer clear differences, apart from the presence of the signal at 3.34 ppm.

The changes observed during freezing affects significantly PC and Cho, and seem also to influence other metabolites (Figs. 2c, 3c), even though at a lesser extent. These findings suggest that care should be used when employing only ChoCC signals for the distinction between neoplastic and healthy tissues or the assessment of tumor grade.

Despite half an hour on ice before freezing, HR-MAS NMR spectra of neoplastic samples remain sufficiently different from those of the healthy one, and they cluster in two groups when PCA is run on CPMG spectra. The differences between healthy and neoplastic tissues, as derived from PCA and PLS-DA, correspond to the enhancement of Lac, Tau, PC, PE, Cr, Asc and a slight enhancement of Gly, and to the lowering of X, Glc and Myo in the neoplastic samples with respect to the healthy ones. The analysis of integrals shows that only changes in Glc, Asc, Lac, Myo, Tau, PC, PE and Cho are statistically significant at a $p < 0.0003$. These results are very close to that observed and already discussed by Bathen et al., with few differences probably due to the spectrometer field (we can hardly resolve Gly from Myo) and to the longer total echo time employed by us.

The use of ROC curves helps in the discrimination between healthy and neoplastic breast tissue. Good biomarkers for the classification seem to be PE, Lac and combinations of Lac, PE, Tau, Myo and Glc. Among these, some ratios, such as Lac + PE + Tau/Glc + Myo, are found in very narrow intervals for healthy samples, well distinguished from the neoplastic ones.

5. Electronic supplementary material

Below is the link to the electronic supplementary material.

Supplementary material 1 (DOC 1309 kb)

References

Ackerstaff, E., Glunde, K., & Bhujwalla, Z. M. (2003). Choline phospholipid metabolism: A target in cancer cells? *Journal of Cellular Biochemistry, 90*, 525–533.

Aoyama, C., Liao, H., & Ishidate, K. (2004). Structure and function of choline kinase isoforms in mammalian cells. *Progress in Lipid Research, 43*, 266–281.

Bathen, F. T., Geurts, B., Sitter, B., Fjøsne, H. E., Lundgren, S., Buydens, L. M., et al. (2013). Feasibility of MR metabolomics for immediate analysis of resection margins during breast cancer surgery. *PLoS ONE, 8*, e61578.

Bathen, F. T., Sitter, B., Sjøbakk, T. E., Tessem, M. B., & Gribbestad, I. S. (2010). Magnetic resonance metabolomics of intact tissue: A biotechnological tool in cancer diagnostics and treatment evaluation. *Cancer Research, 70*, 6692–6696.

Bax, A. (1985). A spatially selective composite 90° radiofrequency pulse. *Journal of Magnetic Resonance, 65*, 142–145.

Brizel, D. M., Schroeder, T., Scher, R. L., Walenta, S., Clough, R. W., Dewhirst, M. W., et al. (2001). Elevated tumor lactate concentrations predict for an increased risk of metastases in head-and-neck cancer. *International Journal of Radiation Oncology Biology Physics, 51*, 349–353.

Cacciatore, S., Hu, X., Viertler, C., Kap, M., Bernhardt, G. A., Mischinger, H. J., et al. (2013). Effects of intra- and post-operative ischemia on the metabolic profile of clinical liver tissue specimens monitored by NMR. *Journal of Proteome Research, 12*, 5723–5729.

Cao, M. D., Sitter, B., Bathen, T. F., Bofin, A., Lønning, P. E., Lundgren, S., et al. (2012). Predicting long-term survival and treatment response in breast cancer patients receiving neoadjuvant chemotherapy by MR metabolic profiling. *NMR in Biomedicine, 25*, 369–378.

Cheng, L. L., Chang, I. W., Smith, B. L., & Gonzalez, R. G. (1998). Evaluating human breast ductal carcinomas with high-resolution magic-angle spinning proton magnetic resonance spectroscopy. *Journal of Magnetic Resonance, 135*, 194–202.

Choi, J. S., Baek, H. M., Kim, S., Kim, J. M., Youk, H. J., Moon, H. J., et al. (2012). HR-MAS MR spectroscopy of breast cancer tissue obtained with core needle biopsy: Correlation with prognostic factors. *PLoS ONE, 7*, e51712.

Elston, C. W., & Ellis, I. O. (1991). Pathologic prognostic factors in breast cancer. The value of histological grades in breast cancer. Experience from a large study with long-term follow-up. *Histopathology, 19*, 403–410.

Esmaeili, M., Moestue, S. A., Hamans, B. C., Veltien, A., Kristian, A., Engebraten, O., et al. (2014). In vivo ^{31}P magnetic resonance spectroscopic imaging (MRSI) for metabolic profiling of human breast cancer xenografts. *Journal of Magnetic Resonance Imaging*. doi:10.1002/jmri.24588.

Federico, M., Artioli, M. E., Braghiroli, B., Cirilli, C., Iachetta, F., Luminari, S., et al. (2013). Regione Emilia Romagna. I tumori nelle province di Modena e Parma; Rapporto novembre 2013; ~~a cura del~~ *Registro tumori della Provincia di Modena* ~~e del~~ *and Registro tumori della Provincia di Parma. 32*, 6–7.

AQ3

Ferlay, J., Soerjomataram, I., Ervik, M., Dikshit, R., Eser, S., Mathers, C., et al. (2013). GLOBOCAN 2012v1.0, Cancer Incidence and mortality Worldwide: IARC CancerBase No 11. Lyon, France: International Agency for Research on Cancer

Ferreira, A. K., Meneguelo, R., Pereira, A., Mendonca, O., Filho, R.,

Chierice, G. O., et al. (2013). Synthetic phosphoethanolamine induces cell cycle arrest and apoptosis in human breast cancer MCF-7 cells through the mitochondrial pathway. *Biomedicine & Pharmacotherapy, 67*, 481–487.

Glunde, K., Bhujwalla, Z. M., & Ronen, S. M. (2011). Choline metabolism in malignant transformation. *Nature Reviews Cancer, 11*, 835–848.

Jain, M., Nilsson, R., Sharma, S., Madhusudhan, N., Kitami, T., Souza, A. L., et al. (2012). Metabolite profiling identifies a key role for glycine in rapid cancer cell proliferation. *Science, 336*, 1040–1044.

Jiang, L., Greenwood, T. R., Artemov, D., Raman, V., Winnard, P. T., Heeren, R. M. A., et al. (2012). Localized hypoxia results in spatially heterogeneous metabolic signatures in breast tumor models. *Neoplasia, 14*, 732–741.

Jordan, K. W., He, W., Halpern, E. F., Wu, C. L., & Cheng, L. L. (2007). Evaluation of tissue metabolites with high resolution magic angle spinning MR spectroscopy human prostate samples after 3-year storage at −80 °C. *Biomarker Insights, 2*, 147–154.

Kinross, J. M., Holmes, E., Darzi, A. W., & Nicholson, J. K. (2011). Metabolic phenotyping for monitoring surgical patients. *Lancet, 377*, 1817–1819.

Li, M., Song, Y., Cho, N., Chang, J. M., Koo, H. R., Yi, A., et al. (2011). An HR-MAS MR metabolomics study on breast tissues obtained with core needle biopsy. *PLoS ONE, 6*, e25563.

Meiboom, S., & Gill, D. (1958). Modified spin-echo method for measuring nuclear relaxation time. *Review of Scientific Instruments, 20*, 688–691.

Moestue, S., Sitter, B., Bathern, T. F., Tessem, M. B., & Gribbestad, I. S. (2011). HR MAS MR spectroscopy in metabolic characterization of cancer. *Current Topics in Medicinal Chemistry, 11*, 2–26.

Opstad, K. S., Bell, B. A., Griffiths, J. R., & Howe, F. A. (2008). An investigation of human brain tumour lipids by high-resolution magic angle spinning ^{1}H MRS and histological analysis. *NMR in Biomedicine, 21*, 1138–1147.

Peeling, J., & Sutherland, G. (1992). High-resolution ^{1}H NMR spectroscopy studies of extracts of human cerebral neoplasms. *Magnetic Resonance in Medicine, 24*, 123–136.

Piotto, M., Moussallieh, F. M., Neuville, A., Bellocq, J. P., Elbayed, K., & Namer, I. J. (2012). Towards real-time metabolic profiling of a biopsy specimen during a surgical operation by ^{1}H high resolution magic angle spinning nuclear magnetic resonance: A case report. *Journal of Medical Case Reports, 6*, 22.

Podo, F. (1999). Tumour phospholipid metabolism. *NMR in Biomedicine, 12*, 413–439.

Quaglia, A., Lillini, R., Crocetti, E., Buzzoni, C., Vercelli, M., & AIRTUM Working Group. (2013). Incidence and mortality trends for four major cancers in the elderly and middle-aged adults: An international comparison. *Surgical Oncology, 22*, e31–e38.

Quennet, V., Yaromina, A., Zips, D., Rosner, A., Walenta, S., Baumann, M., et al. (2006). Tumor lactate content predicts for response to fractionated irradiation of human squamous cell carcinomas in nude mice. *Radiotherapy and Oncology, 81*, 130–135.

Rossi, S., Crocetti, E., Capocaccia, R., Gatta, G., & AIRTUM Working Group. (2013). Estimates of cancer burden in Italy. *Tumori, 2013,* (99), 416–424.

Sitter, B., Lundgren, S., Bathen, T. F., Halgunset, J., Fjosne, H. E., & Gribbestad, I. S. (2006). Comparison of HR MAS MR spectroscopic profiles of breast cancer tissue with clinical parameters. *NMR in Biomedicine, 19*, 30–40.

Sitter, B., Sonnewald, U., Spraul, M., Fjosne, H. E., & Gribbestad, I. S. (2002). High-resolution magic angle spinning MRS of breast cancer

tissue. *NMR in Biomedicine, 15*, 327–337.

Sobin, L. H., Gospodarowicz, M. K., & Wittekind, Ch. (2009). *TNM classification of malignant tumors* (7th ed.). Oxford: Wiley-Blackwell.

Swanson, M. G., Keshari, K. R., Tabatabai, Z. L., Simko, J. P., Shinohara, K., Carroll, P. R., et al. (2008). Quantification of choline- and ethanolamine-containing metabolites in human prostate tissues using ^{1}H HR-MAS total correlation spectroscopy. *Magnetic Resonance in Medicine, 60*, 33–40.

Tavassoli, F. A., & Devilee, P. (Eds.). (2003). *Word Health Organization: Tumor of the breast and female genital organ.* Oxford: Oxford University Press.

Tripathi, P., Kamarajan, P., Somashekar, B. S., MacKinnon, N., Chinnaiyan, A. M., Kapila, Y. L., et al. (2012). Delineating metabolic signatures of head and neck squamous cell carcinoma: Phospholipase A2, a potential therapeutic target. *International Journal of Biochemistry & Cell Biology, 44*, 1852–1861.

Tripathi, P., Somashekar, B. S., Ponnusamy, M., Gursky, A., Dailey, S., Kunju, P., et al. (2013). HR-MAS NMR tissue metabolomic signatures cross-validated by mass spectrometry distinguish bladder cancer from benign disease. *Journal of Proteome Research, 12*, 3519–3528.

Vander Heiden, M. G., Cantley, L. C., & Thompson, C. B. (2009). Understanding the Warburg effect: The metabolic requirements of cell proliferation. *Science, 324*, 1029–1033.

Walenta, S., Wetterling, M., Lehrke, M., Schwickert, G., Sundfør, K., Rofstad, E. K., et al. (2000). High lactate levels predict likelihood of metastases, tumor recurrence, and restricted patient survival in human cervical cancers. *Cancer Research, 60*, 916–921.

Warburg, O. (1956). On the origin of cancer cells. *Science, 123*, 309–314.

Xia, J., Broadhurst, D., Wilson, M., & Wishart, D. S. (2012~~a~~b).

Translational biomarker discovery in clinical metabolomics: An introductory tutorial. *Metabolomics, 9*, 280–299.

Xia, J., Mandal, R., Sinelnikov, I., Broadhurst, D., & Wishart, D. S. (2012a~~b~~). MetaboAnalyst 2.0—a comprehensive server for metabolomic data analysis. *Nucleic Acids Research, 40*, W127–W133.

Xia, J., Psychogios, N., Young, N., & Wishart, D. S. (2009). MetaboAnalyst: A web server for metabolomic data analysis and interpretation. *Nucleic Acids Research, 37*, W652–W660.